Nuclear Instruments and Methods in Physics Research B 97 (1995) 342–345

NIM B
Beam Interactions with Materials & Atoms

ELSEVIER

Plane wave GID topography of defects in lithium niobate after diffusion doping

D.V. Novikov [a,*], T. Gog [a], M. Griebenow [a], G. Materlik [a], I. Baumann [b], W. Sohler [b]

[a] *HASYLAB at DESY, Postfach 22607, Hamburg, Germany*
[b] *Universität – GH Paderborn, 33098 Paderborn, Germany*

Abstract

Grazing-incidence diffraction (GID) synchrotron radiation X-ray topography was used for a depth-resolved investigation of the defect structure of $LiNbO_3$ after surface diffusion doping. Lattice and misfit dislocations as well as strain fields were detected. The method is shown to be effective even for strongly damaged crystals and offers significant advantages for characterization of single crystals and non-perfect epitaxial films.

1. Introduction

X-ray Bragg case topography is widely employed as a non-destructive technique for imaging defects in large single crystals. Its depth resolution is hard to control and usually limited by linear absorption, which for conventional geometries has the order of tens of micrometers. Modern technological developments require analysis of thin surface layers, often with a high density of defects. This problem can be solved by GID topography – a novel method for depth-resolved investigation of near surface defect structure in single crystals [1–5]. In a one crystal variant it can be carried out both with the help of conventional sources and synchrotron radiation (SR) and gives qualitative information about structure perfection of thin surface layers. Plane wave topography, which provides quantitative information, requires multi-crystal arrangements and can be carried out in GID geometry only on synchrotron radiation sources. Making use of extremely asymmetric diffraction geometries, it allows to combine the imaging properties of X-ray diffraction topography with a variation of information depth from about a micrometer down to tens of nanometers, controlled by refraction of the incident beam.

This method requires angles of incidence of the X-rays on the surface to be of the order of the critical angle of total external reflection. Simultaneously, the Bragg diffraction conditions for lattice planes of the crystal must be satisfied. The practical implementation of the method can be carried out in two geometries – a non-coplanar, when the surface normal lies outside the diffraction plane, and a coplanar, where the normal lies in it. The former can be carried out practically on any crystal by choosing a Bragg cone, which intersects the surface, but it involves complicated alignment procedures and produces strong geometrical distortions in the pictures obtained. The latter can be carried out generally only with the tunability of synchrotron radiation. Varying the wavelength of the incident X-rays, one can easily adjust the angle with the surface preserving simultaneously the Bragg diffraction condition.

2. Experiment

The GID topography was used to investigate diffusion doped lithium niobate, a material of great interest for integrated optics [6,7]. The samples studied started from commercially available wafers. Er and Ti surface diffusion doping was carried out by subsequent indiffusion of evaporated layers of Er (thickness 13 nm) and Ti (thickness 95 nm) at 1100°/100 h and 1030°C/9 h, respectively. Only parts of the sample surface were subject to diffusion (see Fig. 1), in order to investigate stress relaxation between the neighboring doped and undoped regions and to compare the results with those, obtained by selective etching. Depth profiles of dopant concentration were analysed with SIMS. For comparison pure wafers were annealed at identical conditions to study a possible dislocation structure evolution.

The experiments were performed at beamlines ROEMO I and CEMO at HASYLAB with a double crystal monochromator, with the first symmetric Ge and the second asymmetric Si crystals. The oblique $(01.\bar{4})$ and $(01.\bar{8})$ planes were used in skew noncoplanar and coplanar geom-

* Corresponding author. Tel. +49 40 8998 3125, fax +49 40 8998 2787, e-mail nowikow@vxdesy.desy.de.

SSDI 0168-583X(94)00717-9

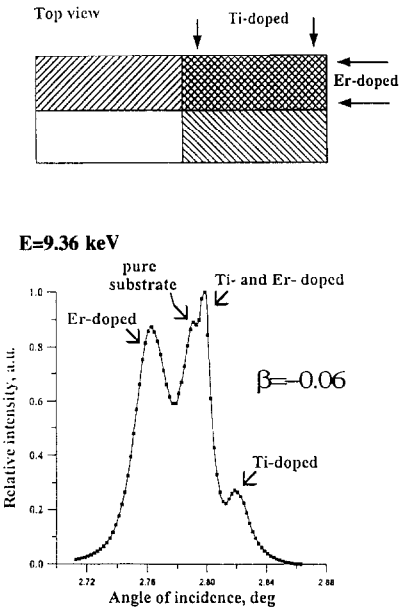

Fig. 1. X-ray reflection curve, $(01.\bar{8})$ diffraction planes and the scheme of the sample.

etry respectively. A variation of asymmetry from $b = -0.06$ to -0.005 and, consequently, a variation of X-ray penetration depth from $\sim$ 2 μm to 200 nm, was achieved.

3. Results and discussion

Lithium niobate single crystals appeared to be significantly damaged by diffusion induced mechanical strain. The diffraction curve Fig. 1 is taken at asymmetric diffraction conditions from a sample with overlapping Er and Ti diffused zones, so that the surface was divided in four parts: undoped bulk material, Ti, Er and Er + Ti doped zones with sharp boundaries between them. The curve reveals four maxima, corresponding to the four different surface areas. The lattice parameter variation $\Delta d/d$, $d(0.\bar{8}) = 0.1615$ nm, with respect to undoped lithium niobate is $(+1.5 \pm 0.2) \times 10^{-3}$, $(-1.9 \pm 0.2) \times 10^{-3}$ and $(+0.6 \pm 0.2) \times 10^{-3}$ for Er, Ti and Er + Ti doped zones respectively, the penetration depth being about 1.6 μm. Decreasing the angle of incidence and, therefore, the depth probed to 0.4 μm, the parameters change to $(+1.8 \pm 0.2) \times 10^{-3}$ for Er and $(-1.8 \pm 0.2) \times 10^{-3}$ for Ti areas. One should mention, that the values are averaged over an 4×4 mm area and do not give absolute values of local impurity induced lattice parameter variation.

Fig. 2a shows a topogram, taken at the maximum of the Ti + Er peak of the curve Fig. 1, which is dominated by basal (00.1) $\langle 1\bar{2}.0 \rangle$ dislocations, not present in the virgin material. They lie parallel to the z-cut surface of the sample. A set of dislocations in the middle of the undoped zone was produced by indentation. They are situated directly under the surface plane and do not differ from the ones introduced by the technological treatment. The area doped with Er shows a structure typical for a very high density of defects, which can not be resolved any further. This must be connected with a high concentration of dopant in the surface layer, 0.11 at.%. Diffusion of Ti over Er leads to the formation of a new surface layer, seen in SIMS curves as a drastical, up to 0.5 at.%, i.e. far over the solubility in lithium niobate, increase of Er concentration at depths to about 150 nm (Fig. 2b). A cloud-like topographical image of this area is characteristic for a material with a very high concentration of point defects. The dislo-

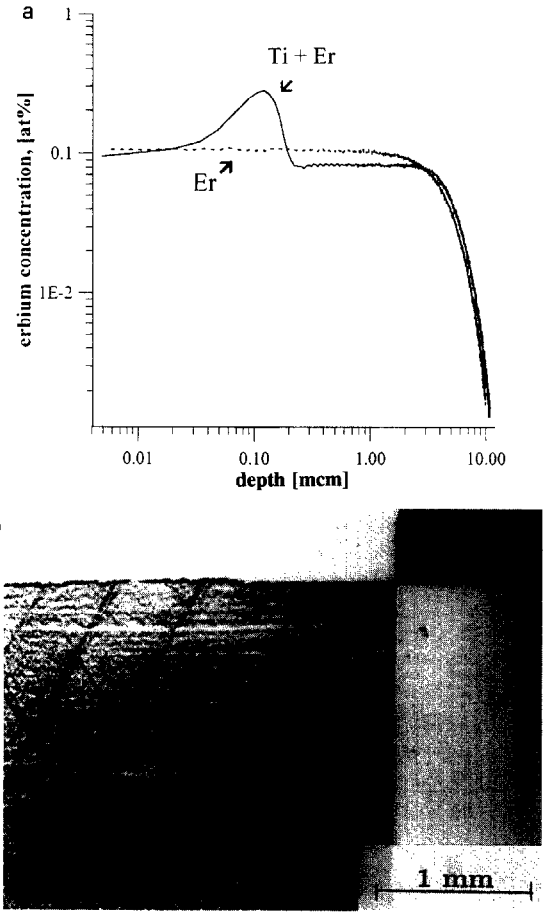

Fig. 2. (a) Asymmetric plane wave SR topogram of the sample at the right slope of the substrate peak (Fig. 1). Information depth 1.6 μm. Three intersecting screw basal (00.1) $\langle 1\bar{2}.0 \rangle$ dislocation sets in the middle of the undoped zone were induced by mechanical indentation. The diffraction vector at all topograms lies along the Ti/undoped substrate boundary. (b) SIMS erbium concentration profiles for Er and Er + Ti doped zones. Diffusion of Ti after Er leads to a formation of a surface Er-enriched layer, which should lead to a formation of a new phase at depths of about 150 nm.

cation structures in the Ti diffused zone do not differ greatly from those for the undoped region, although they show more dislocation systems.

The boundaries between the neighboring zones with different dopants are well resolved and include misfit dislocations (Fig. 3a), giving a contrast with a period of about 20 μm. A low-angle boundary running across the misfit dislocation system does not cause visible changes in it.

In the topograms at smaller penetration depths new types of defect images appear. The topogram of the Ti doped zone with an information depth about 0.4 μm is crossed by a series of parallel and curved lines, caused by mechanical deformations (Fig. 3b). A further decrease of glancing angle decreases the number of features seen in the image, which is connected with the smaller depth probed and also with an inevitable loss of lattice parameter resolution (Fig. 4a). The images of the defects next to the surface display no qualitative changes, while those of the bulk become blurred. It is clearly seen, that near the border between Ti/Er + Ti zones the strain relaxes elastically and provides a long-range field. On the contrary, in the Er/undoped $LiNbO_3$ transition area no strain contrast can be seen. It corresponds to the results of etching, which depicts pile-ups of lattice dislocation in this area (Fig. 4b).

The total bending of the samples, presenting a serious problem for usual topography techniques, did not have any noticeable influence in GID geometry.

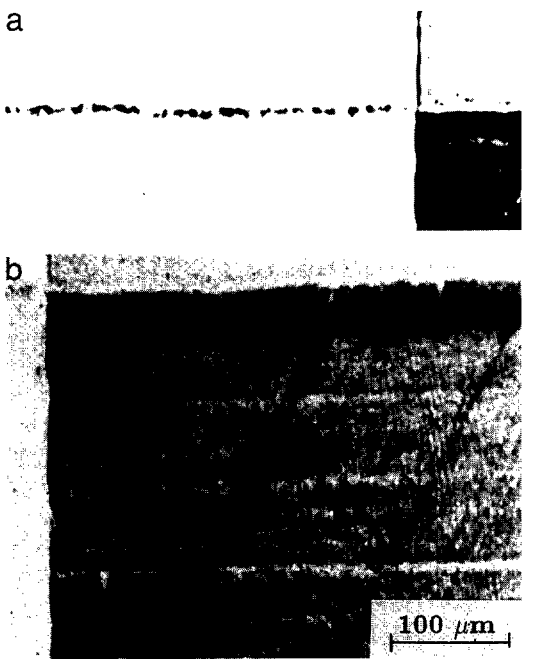

Fig. 3. (a) Er/undoped substrate misfit dislocations. Topogram taken at the right slope of the Ti zone peak; (b) Plane wave GID topogram of Ti area. Information depth 0.4 μm. New quasiperiodic images normal to the Er + Ti/Er boundary are resolved.

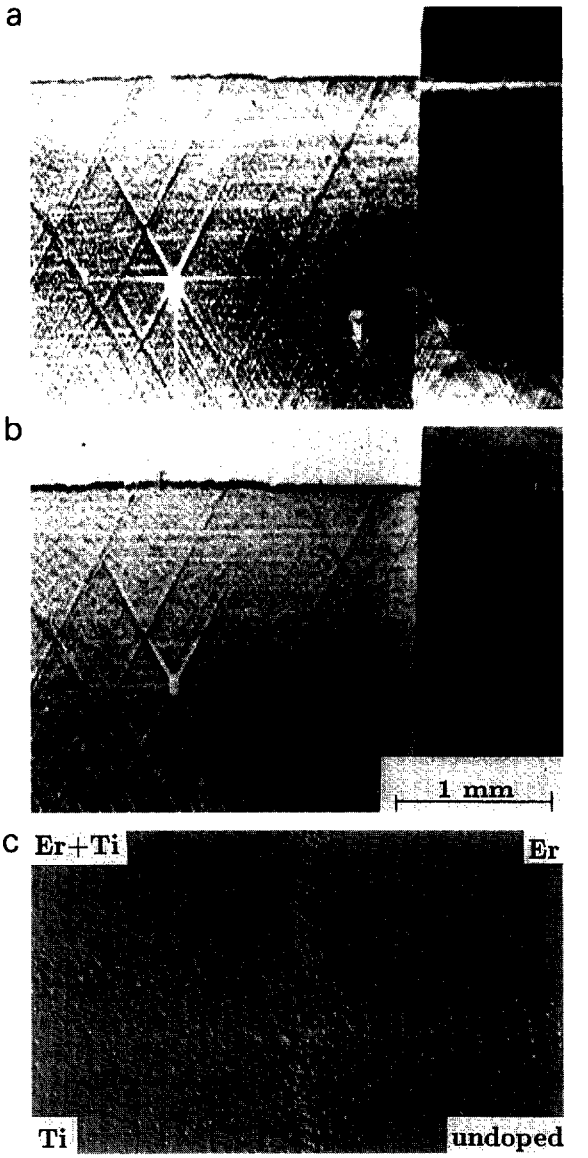

Fig. 4. (a,b) Extreme GID plane wave topograms, obtained respectively on the right and on the left slopes of the diffraction curve. Information depth about 200 nm. Contrast variation from the strain field at the Er + Ti/Ti boundary is observed. (c) Microphotograph of the sample surface after selective etching in $HF:HNO_3$ (1:2) solution. The pile-ups of dislocation are seen on the Er/undoped material boundary and are absent on the Er/Ti + Er one.

4. Conclusion

GID topography provides all the features of usual asymmetric geometries while having strong advantages for surface defect analysis, combining higher depth resolution

with less sensitivity to the quality of the underlying bulk material.

With the transition to grazing incidence and, therefore, to lower penetration depth, the resolution of surface elements in the image becomes higher, while the underlying structures disappear. At the same time, all the parts of the sample begin to give a strong diffraction scattering simultaneously, so that different parts with large, 10^{-3}, lattice parameter difference, can be imaged simultaneously. This is a great advantage for investigation of materials of low perfection or thin films on such substrates.

It is shown, that surface diffusion doping of $LiNbO_3$, used for production of optoelectronic devices, can significantly damage the crystal and leads to formation of lattice and misfit dislocations and strong long range elastic strain fields near the diffusion zones.

References

[1] T. Kitan, T. Ishikawa, J. Matsui, K. Akimoto, J. Mizuki and Y. Kawase, Jpn. J. Appl. Phys. 26 (1987) L108.
[2] R.M. Imamov, A.A. Lomov and D.V. Novikov, Phys. Status. Solidi A 115 (1989) K133.
[3] M. Dudley, J. Wu and G.-D. Yao, Nucl. Instr. and Meth. B 40/41 (1989) 388.
[4] M. Griebenow, T. Gog, G. Materlik and W. Sohler, HASYLAB Jahresbericht (1992) p. 335.
[5] S. Kimura, J. Harada and T. Ishikawa, Acta Crystallogr. A 50 (1994) 337.
[6] H. Suche, I. Baumann, D. Hiller and W. Sohler, Electron. Lett. 29 (1993) 1111.
[7] R. Brinkmann, I. Baumann, M. Dinand, W. Sohler and H. Suche, IEEE J. Quantum Electron. QE-30 (1994), in press.